Synaptic activity prompts γ-secretase–mediated cleavage of EphA4 and dendritic spine formation

Eiji Inoue,[1] Maki Deguchi-Tawarada,[1] Aki Togawa,[1] Chiyuki Matsui,[1] Kohei Arita,[1] Sayaka Katahira-Tayama,[1] Toshitaka Sato,[2] Emiko Yamauchi,[2] Yoshiya Oda,[2] and Yoshimi Takai[3]

[1]KAN Research Institute, Kobe 650-0047, Japan
[2]Laboratory of Core Technology, Eisai Co., Ltd., Ibaraki 300-2635, Japan
[3]Division of Molecular and Cellular Biology, Department of Biochemistry and Molecular Biology, Kobe University Graduate School of Medicine, Kobe 650-0017, Japan

Alzheimer's disease is an age-dependent neurodegenerative disorder that is characterized by a progressive decline in cognitive function. γ-secretase dysfunction is evident in many cases of early onset familial Alzheimer's disease. However, the mechanism by which γ-secretase dysfunction results in memory loss and neurodegeneration is not fully understood. Here, we demonstrate that γ-secretase is localized at synapses and regulates spine formation. We identify EphA4, one of the Ephrin receptor family members, as a substrate of γ-secretase, and find that EphA4 processing is enhanced by synaptic activity. Moreover, overexpression of EphA4 intracellular domain increases the number of dendritic spines by activating the Rac signaling pathway. These findings reveal a function for EphA4-mediated intracellular signaling in the morphogenesis of dendritic spines and suggest that the processing of EphA4 by γ-secretase affects the pathogenesis of Alzheimer's disease.

Introduction

Alzheimer's disease is an age-dependent, progressive dementia, which is clinically characterized by impaired memory, cognition, and behavior. Pathologically, Alzheimer's disease is distinguished by the presence of neurofibrillary tangles and β-amyloid–containing senile plaques in the neocortex and hippocampus. However, several studies have shown the presence of neurofibrillary tangles and senile plaques in the neocortex and hippocampus of nondemented, elderly individuals (Arriagada et al., 1992; Kazee and Johnson, 1998). It has been shown that the extent of synaptic loss is correlated with impaired cognitive functions during the early and late stages of Alzheimer's disease (Scheff et al., 2006). Therefore, in addition to neurofibrillary tangles and senile plaques, abnormal formation and maintenance of synapses have been considered to contribute to the pathogenesis of Alzheimer's disease.

Presenilin (PS) functions as part of γ-secretase, a multisubunit protease complex containing at least three other transmembrane proteins, namely Nicastrin, Aph-1, and Pen-2. It has been demonstrated that mutations in the PS gene are responsible for many cases of early onset familial Alzheimer's disease (De Strooper, 2003). PS is the catalytic subunit of γ-secretase, and is composed of two closely related family members, PS1 and PS2. PS is ubiquitously expressed in peripheral tissues, as well as in the central nervous system. Although several studies using cultured neurons or nonneuronal cell lines have demonstrated that γ-secretase is localized in intracellular membranes, such as the Golgi apparatus (Annaert et al., 1999; Rechards et al., 2003), PS1 has also been found to associate with synaptic vesicles and synaptic plasma membranes in the brain (Beher et al., 1999). Moreover, PS1 was found to associate with the *N*-methyl-D-aspartic acid (NMDA) receptor (Saura et al., 2004). Thus, γ-secretase is thought to localize and function at synapses, but the precise localization and physiological function of γ-secretase in neurons remain elusive.

γ-secretase is responsible for the intramembranous cleavage of amyloid-precursor protein. After ectodomain shedding by β-secretase, γ-secretase cleaves amyloid precursor protein in the transmembrane region, generating a β-amyloid peptide and a soluble peptide containing the cytoplasmic region (Landman and Kim, 2004). The resulting soluble peptide is the so-called "intracellular domain" (ICD) of amyloid precursor protein, which has been

Correspondence to Eiji Inoue: e-inoue@kan.eisai.co.jp

Abbreviations used in this paper: AMPA, α-amino-3-hydroxy-5-methyl-4–isoxazolepropionic acid; CTF, C-terminal fragment; DIV, day in vitro; GluR1, glutamate receptor 1; ICD, intracellular domain; MMP, matrix metalloprotease; NMDA, *N*-methyl-D-aspartic acid; PS, presenilin.

The Rockefeller University Press $30.00
J. Cell Biol. Vol. 185 No. 3 551–564
www.jcb.org/cgi/doi/10.1083/jcb.200809151

known to function as a gene transcription regulator (Landman and Kim, 2004). Familial Alzheimer's disease-linked mutations of PS lead to enhanced release of the amylogenic 42-residue peptide, which has toxic effects on various neuronal functions. Studies have suggested that toxic γ-secretase gain-of-function is responsible for the pathogenesis of Alzheimer's disease (Walsh and Selkoe, 2004). However, it has been shown that familial Alzheimer's disease-linked PS mutations impair the processing of various substrates, resulting in reduced ICDs from these substrates (Moehlmann et al., 2002; Bentahir et al., 2006). These ICD-mediated signaling pathways are involved in various neuronal functions (Landman and Kim, 2004). Moreover, conditional PS1/PS2 double knockout mice exhibit age-dependent progressive memory loss and neurodegeneration resembling Alzheimer's disease (Saura et al., 2004). These findings suggest that the regulation of ICD signaling by γ-secretase has a critical role in synaptic plasticity and could, therefore, be involved in the pathogenesis of Alzheimer's disease.

To investigate the physiological function of γ-secretase at synapses, we attempted to identify novel substrates of γ-secretase. In the present study, we demonstrate that EphA4 is processed by γ-secretase, and that the processing of EphA4 enhances the formation and maintenance of dendritic spines through activation of the Rac signaling pathway.

Results

Localization of γ-secretase in hippocampal neurons

To determine the localization of γ-secretase in the mouse hippocampus, we compared the localization of PS1 with those of various synaptic markers. In the hippocampal CA3 region, the immunofluorescence signal for PS1 revealed a dot-like pattern in the stratum lucidum, the region where synapses are formed between mossy fiber terminals and the dendrites of pyramidal cells. The signals partly overlapped with those of the postsynaptic protein Homer and active zone protein Bassoon (Fig. 1 A). In rat hippocampal primary cultured neurons, the signals for PS1 exhibited a dot-like pattern along dendrites and partly colocalized with those of Homer and Bassoon (Fig. 1 B). These results suggest that γ-secretase localizes at synapses.

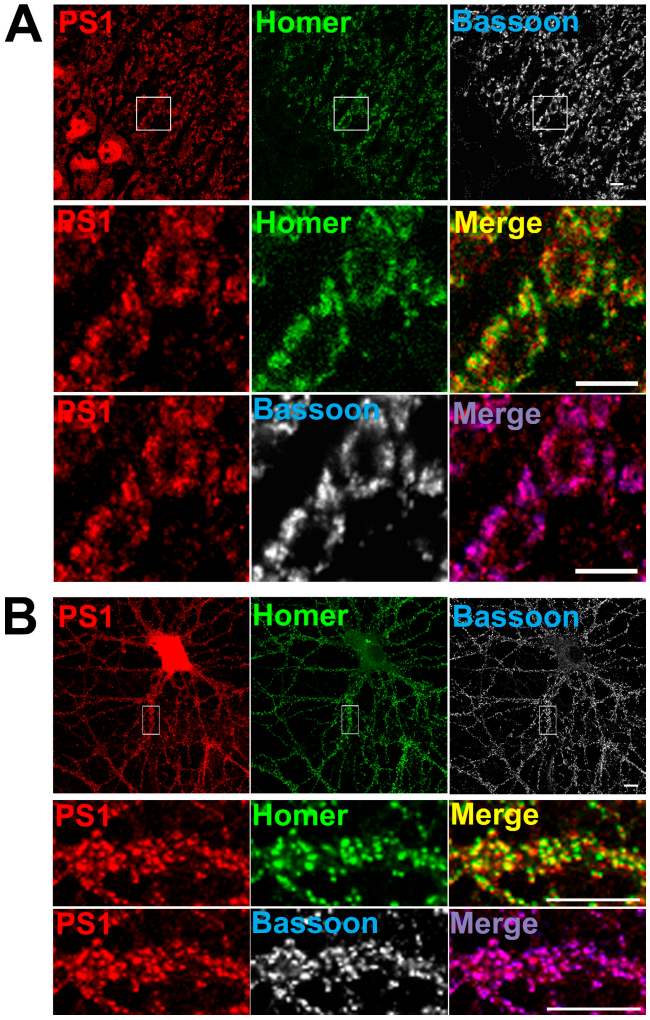

Figure 1. **Localization of PS1 in mouse hippocampal tissues and rat hippocampal primary cultured neurons.** (A) Immunofluorescence microscopy of the mouse hippocampal CA3 region. Sections were triple-stained with the anti-PS1, the anti-Homer, and the anti-Bassoon antibodies. (B) Localization of PS1 in rat hippocampal primary cultured neurons. Neurons at 21 d of culture were fixed and triple-stained with the anti-PS1, the anti-Homer, and the anti-Bassoon antibodies. The bottom two rows in each panel show enlarged views of the boxed regions above. The results represent three independent experiments. Bars, 10 μm.

Physiological function of γ-secretase in the formation of dendritic spines

Clustering of the α-amino-3-hydroxy-5-methyl-4-isoxazole-propionic acid (AMPA) receptor at synapses is a critical step for functional maturation of excitatory synapses (Derkach et al., 2007). To address the physiological function of γ-secretase at synapses, we first examined the effect of a γ-secretase inhibitor (compound E) on the clustering of the AMPA receptor. Rat hippocampal primary cultured neurons were treated with compound E from day in vitro (DIV) 14 to 21. Subsequently, the localizations of the AMPA receptor subunit, glutamate receptor 1 (GluR1), and synaptophysin were determined by immunocytochemistry. The density of GluR1 clusters was reduced by ∼25% in neurons treated with compound E (control vs. compound E: 4.16 ± 0.30 vs. 3.09 ± 0.26 puncta/10 μm dendrite; $P < 0.05$; Fig. 2, A and B). The clustering of synaptophysin, however, was not affected by compound E (Fig. 2, A and B). We then analyzed the localization of another postsynaptic protein, PSD-95, a well-known protein that regulates postsynapse development (Kim and Sheng, 2004). The number of PSD-95 clusters was not affected by compound E (Fig. 2, A and B). However, the size of the PSD-95 clusters was slightly enlarged (control vs. compound E: 0.114 ± 0.002 vs. 0.135 ± 0.004 μm^2; $P < 0.01$; Fig. 2 A). We then examined the effect of compound E on the morphology of dendritic spines. To visualize the shapes of dendritic spines, rat hippocampal primary cultured neurons were transfected with GFP at DIV 9. The neurons were treated with compound E from DIV 14 to 21, and then analyzed at DIV 21. The density of dendritic spines, defined as protrusions, was reduced by ∼20% compared with neurons treated with DMSO (control vs. compound E: 6.43 ± 0.33 vs. 5.35 ± 0.22 protrusions/10 μm dendrite; $P < 0.05$; Fig. 2, C and D). The mean length and width of the remaining spines were not affected by compound E (Fig. 2, C and D).

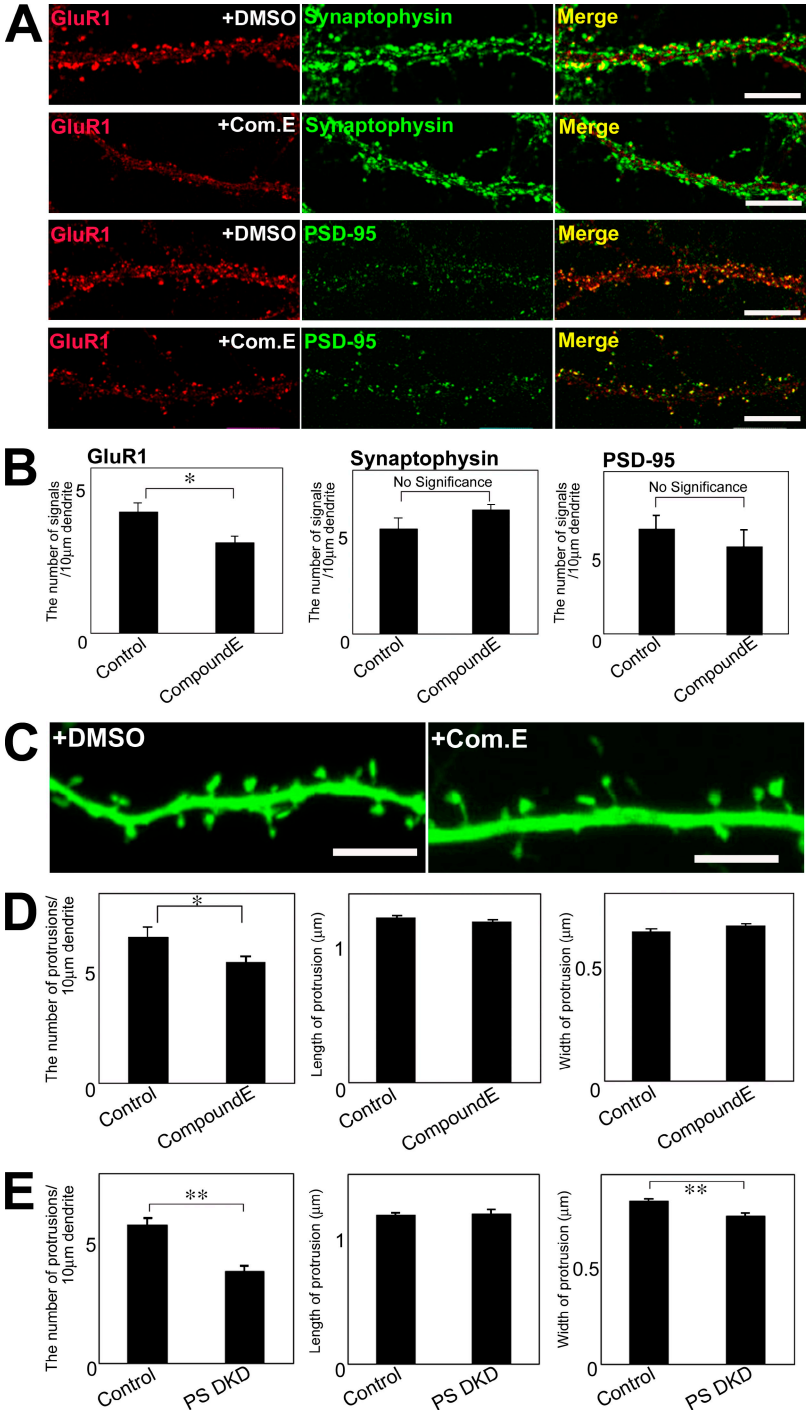

Figure 2. **Effect of γ-secretase inhibitor on spine morphology.** (A) Immunofluorescence microscopy. Neurons at DIV 14 were treated with DMSO or compound E for 1 wk, and then double-stained with the anti-GluR1 and anti-synaptophysin or PSD-95 antibodies. Com. E, compound E. Bars, 10 μm. (B) Quantitative analysis of the effects of compound E on the localizations of GluR1, synaptophysin, and PSD-95. (C) Immunofluorescence microscopy. Neurons at DIV 9 were transfected with GFP, and treated with DMSO or compound E at DIV 14. The neurons were further incubated for 1 wk, and then stained with the anti-GFP antibody. Bars, 5 μm. (D) Quantitative analysis of the effect of compound E on the morphology of dendritic spines. (E) Quantitative analysis of the effect of PS double knockdown on the morphology of dendritic spines. DKD, double knockdown. The results represent three independent experiments. Data are expressed as means ± SEM. **, $P < 0.01$; *, $P < 0.05$.

We further examined the effect of double knockdown of PS1 and PS2 on the morphogenesis of dendritic spines. We prepared RNAi constructs against PS1 and PS2, and confirmed that these RNAi constructs specifically reduced the expressions of the PSs and the activity of γ-secretase (Fig. S1). Rat hippocampal primary cultured neurons were transfected with these RNAi constructs at DIV 13 and analyzed at DIV 21. Similar to the effect of the γ-secretase inhibitor, the number of dendritic spines was decreased by ~30% compared with control neurons (control vs. PS double knockdown: 5.57 ± 0.28 vs. 3.68 ± 0.25 puncta/10 μm dendrite; $P < 0.01$; Fig. 2 E). In addition, the mean width of the remaining spines was slightly diminished by PS double knockdown (width of protrusion for control vs. PS double knockdown: 0.93 ± 0.02 vs. 0.85 ± 0.02 μm; $P < 0.01$; Fig. 2 E). Collectively, these results indicate that γ-secretase is involved in the formation and maintenance of dendritic spines.

Identification of EphA4 as a substrate of γ-secretase

To elucidate the physiological role of γ-secretase in the formation of dendritic spines, we attempted to identify its substrates. Several substrates have been demonstrated to codistribute with

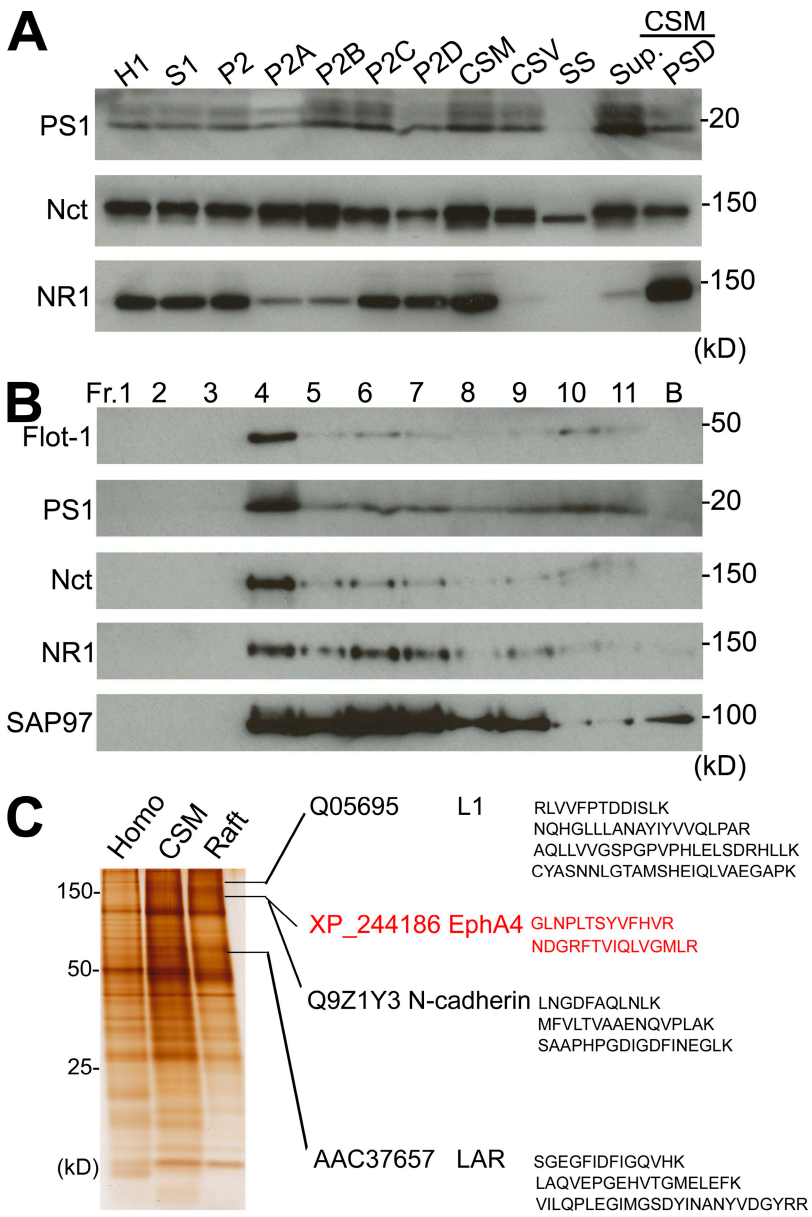

Figure 3. **Identification of γ-secretase substrates.** (A) Subcellular distribution. Rat brain homogenates were subjected to subcellular fractionation. An aliquot of each fraction (5 µg of each protein) was analyzed by Western blotting using the indicated antibodies. H1, homogenate; S1, crude synaptosome fraction; P2, crude membrane fraction; P2A, myelin fraction; P2B, ER, Golgi complex, and membranes fraction; P2C, synaptosome fraction; P2D, mitochondria fraction; CSM, crude synaptic membrane fraction; CSV, crude synaptic vesicle fraction; SS, synaptic cytosol fraction; Sup, 1% Triton X-100–soluble fraction of CSM; PSD, 1% Triton X-100–insoluble fraction of CSM (postsynaptic density fraction); Nct, Nicastrin; NR1, NMDA receptor 1. (B) Association of γ-secretase with the synaptic lipid raft membrane. The purified CSM fraction was treated with 0.5% Lubrol, followed by sucrose density gradient centrifugation. After centrifugation, fractions (1 ml each) were taken from the layers and analyzed by Western blotting using the indicated antibodies. Flot-1, Flotillin-1. (C) Silver staining of the homogenate, CSM, and synaptic lipid raft membrane fractions. Equal amounts of the individual fractions were subjected to SDS-PAGE, followed by silver staining.

γ-secretase within the same membrane compartment in the brain (Kamal et al., 2001). These findings led us to speculate that the physiological substrates could be associated with specific membrane compartments where γ-secretase becomes concentrated. We first examined the subcellular distributions of various γ-secretase components. PS1 and Nicastrin were broadly distributed and relatively concentrated in the crude synaptic membrane fraction, where many presynaptic and postsynaptic membrane proteins, such as NMDA receptor, were concentrated (Fig. 3 A). These results support the notion that γ-secretase localizes at synapses.

It has been demonstrated that γ-secretase is concentrated in the lipid raft membrane (Vetrivel et al., 2004). In hippocampal neurons, the lipid raft membrane exists in dendritic spines and regulates AMPA receptor trafficking (Hering et al., 2003). Therefore, we purified the lipid raft membrane from the crude synaptic membrane fraction and examined the distributions of γ-secretase components. Western blot analysis revealed that PS1 and Nicastrin were concentrated in fraction 4, where Flotillin-1, a well-known lipid raft marker (Bickel et al., 1997), was concentrated (Fig. 3 B). In addition, NMDA receptor 1, but not SAP97 that does not associate with the synaptic lipid raft (Hering et al., 2003), was concentrated in the same fraction, which suggests that γ-secretase is concentrated in the synaptic lipid raft membrane.

The purified synaptic lipid raft membrane proteins were separated by SDS-PAGE and subjected to silver staining (Fig. 3 C). The band pattern of the purified synaptic lipid raft membrane fraction varied from the original crude synaptic membrane fraction (Fig. 3 C). To identify possible substrates, we attempted to identify all the components in the synaptic lipid raft membrane fraction. The entire lane was divided into 18 segments, followed by in-gel Lys-C and trypsin digestion. The resulting peptides from each segment were analyzed by nano flow liquid chromatography tandem mass spectrometry (Tabata et al., 2007). As a result, we identified 324 proteins from the purified synaptic lipid raft membrane fraction. L1, *N*-cadherin, and LAR, which are previously known substrates (Marambaud et al., 2003; Maretzky

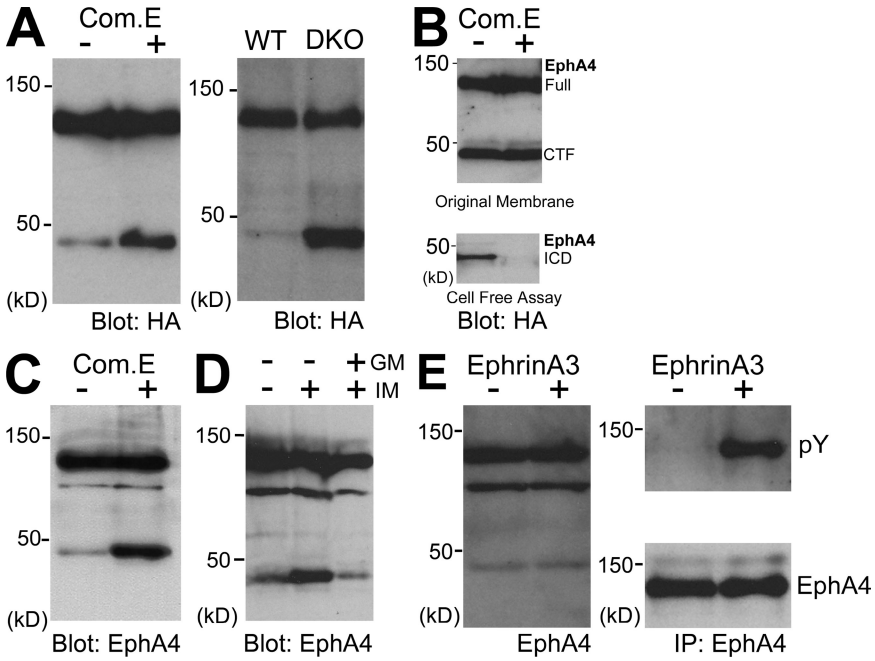

Figure 4. **Processing of EphA4 by MMP and γ-secretase.** (A) Processing of exogenously expressed EphA4 by γ-secretase. (A, left) HEK293 cells were transfected with EphA4-HA, followed by treatment with DMSO or compound E for 1 d. The cells were then extracted and analyzed by Western blotting using the anti-HA antibody. Com. E, compound E. (A, right) PS1/PS2 double knockout cells were transfected with EphA4-HA, followed by Western blotting using the anti-HA antibody. (B) In vitro γ-secretase assay. Membrane fractions purified from EphA4-HA–expressing HEK293 cells were incubated in the presence or absence of compound E for 16 h. The fractions were then separated into membrane and buffer fractions containing the generated ICD. The ICD was purified by immunoprecipitation using the anti-HA antibody, followed by Western blotting. (C) Processing of endogenous EphA4 by γ-secretase in rat hippocampal primary cultured neurons. Neurons were treated with DMSO or compound E at DIV 14. The neurons were further incubated for 1 wk, followed by Western blotting using the anti-EphA4 antibody. (D) Stimulation of the processing of EphA4 by ionomycin. Neurons were treated with DMSO or 10 μM ionomycin in the presence or absence of GM6001 for 30 min, followed by Western blotting using the anti-EphA4 antibody. IM, ionomycin; GM, GM6001. (E) Effect of ligand stimulation on the processing of EphA4. Neurons were treated with 10 μg/ml Fc or EphrinA3-Fc for 2 h in the presence of compound E. EphA4 was immunoprecipitated with the anti-EphA4 antibody and analyzed by Western blotting using the anti-EphA4 and the anti–phospho-tyrosine antibodies. pY, phospho-tyrosine.

et al., 2005; Haapasalo et al., 2007), were included in this fraction. In addition to these substrates, EphA4 was included in the synaptic lipid raft membrane fraction (Fig. 3 C). EphA4 has a lysine/arginine-rich motif in the juxtamembrane region, which is the consensus motif for the substrates of γ-secretase (Haapasalo et al., 2007).

Processing of EphA4 by MMPs (matrix metalloproteases) and γ-secretase

We examined whether EphA4 was processed by γ-secretase. Ectodomain shedding of the substrate is required for γ-secretase–mediated substrate cleavage (Landman and Kim, 2004). Therefore, inhibition of γ-secretase activity results in accumulation of the intermediate C-terminal fragment (CTF), which is generated by ectodomain shedding of the substrate (Haapasalo et al., 2007). HEK293 cells were transfected with EphA4-HA and treated with compound E. Western blot analysis revealed that a ~50-kD band, corresponding to the CTF, accumulated in cells treated with compound E (Fig. 4 A, left). Similarly, EphA4 CTF accumulated in PS1/PS2 double knockout cells (Herreman et al., 1999; Herreman et al., 2003), but not in wild-type cells (Fig. 4 A, right). We then performed an in vitro γ-secretase assay using the membrane fraction from HEK293 cells expressing EphA4-HA. Western blot analysis revealed that a significant amount of EphA4 ICD was released from the purified membrane fraction, and that the production of EphA4 ICD was completely inhibited by compound E (Fig. 4 B). We further examined whether endogenous EphA4 was processed by γ-secretase in neurons. Rat hippocampal primary cultured neurons were treated with compound E from DIV 14–21. The neurons were extracted, and analyzed by Western blotting using an anti-EphA4 antibody, which is specific for the cytoplasmic region. EphA4 CTF was found to be significantly accumulated in the neurons treated with compound E (Fig. 4 C).

Several substrates of γ-secretase are cleaved in the ectodomain by MMP, which is activated by Ca^{2+} influx (Litterst et al., 2007). To determine whether MMP processes EphA4, rat hippocampal primary cultured neurons were treated with the calcium ionophore ionomycin, which resulted in a rapid increase in CTF (Fig. 4 D). Moreover, the MMP inhibitor GM6001 was capable of inhibiting the ionomycin-induced increase in CTF, indicating that ectodomain cleavage of EphA4 is mediated by MMP. Ligand binding is known to stimulate ectodomain cleavage in several substrates, such as Notch, EphrinB, and EphB2 (Le Borgne et al., 2005; Georgakopoulos et al., 2006; Litterst et al., 2007). Treatment with EphrinA3 is reported to stimulate the activation of EphA4 in hippocampal neurons (Murai et al., 2003). Therefore, rat hippocampal primary cultured neurons were treated with an EphrinA3-Fc fusion protein for 2 h in the presence of compound E to determine the effect of EphrinA3 on the MMP-mediated ectodomain cleavage of EphA4. Although EphrinA3-Fc stimulated the phosphorylation of EphA4, the processing of EphA4 was not affected (Fig. 4 E). Furthermore, the processing of EphA4 was not affected by longer treatment with EphrinA3 (16 h; unpublished data). These results suggest that the MMP-mediated ectodomain cleavage of EphA4 is independent of ligand stimulation.

Regulation of the processing of EphA4 by synaptic activity

Inactivation of γ-secretase by conditional PS1/PS2 double knockout has been found to impair long-term potentiation (Saura et al., 2004). These findings suggest that synaptic activation

stimulates the processing of EphA4. Brief applications of reagents that elevate cAMP and increase spontaneous synaptic activity have been shown to increase clustering of the AMPA receptor and induce long-term potentiation (Otmakhov et al., 2004; Kopec et al., 2006). Therefore, we examined the effects of an adenylate cyclase activator (forskolin), a phosphodiesterase inhibitor (rolipram), and a GABA receptor antagonist (bicuculline) on the processing of EphA4. Treatment with forskolin and rolipram enhanced the processing of EphA4, whereas no effect was detected for bicuculline (Fig. 5 A, top left). However, addition of bicuculline to forskolin and rolipram further enhanced the processing of EphA4 (Fig. 5 A, top left). Consistent with a previous study (Oh et al., 2006), the phosphorylation of GluR1 serine 845, which is important for clustering of the AMPA receptor on the cell surface, was increased by this treatment (Fig. 5 A, second panel from the top). To confirm whether the effects of these reagents were mediated by activation of glutamate receptors, we examined the effects of AP5, an NMDA receptor antagonist, and CNQX, an AMPA receptor antagonist. Both AP5 and CNQX inhibited the enhancement of the processing of EphA4, whereas the effect of CNQX was slightly smaller than that of AP5 in the neurons treated by forskolin, rolipram, and bicuculline (Fig. 5 A, bottom two panels). These results indicate that the enhancement of the processing of EphA4 is mediated by activation of glutamate receptors.

As described above, EphA4 was included in the synaptic lipid raft membrane (Fig. 3 C). To examine where EphA4 is processed, we analyzed the subcellular distribution of EphA4 CTF that is generated by MMP. The results revealed that EphA4 CTF, which was increased by synaptic activity, was concentrated in the fraction where Flotillin-1 and NMDA receptor 1 were concentrated (Fig. 5 B). This finding suggests that EphA4 is processed at the synaptic lipid raft membrane.

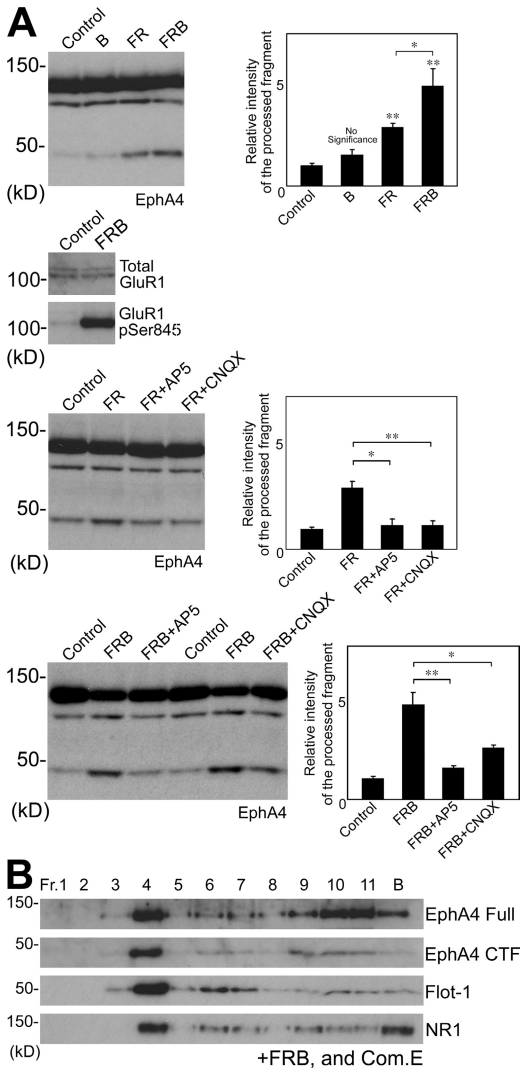

Figure 5. **Synaptic activity–dependent processing of EphA4.** (A) Enhancement of the processing of EphA4 by synaptic activity. (A, top) Effects of forskolin, rolipram, and bicuculline on the processing of EphA4. Neurons were treated with forskolin, rolipram, and bicuculline for 16 h, followed by Western blotting using the anti-EphA4 antibody. (A, second panel from the top) Phosphorylation of GluR1. The lysate was analyzed by Western blotting using the anti-GluR1 and the anti–phospho-GluR1 antibodies. (A, bottom two panels) Effects of AP5 and CNQX on the enhanced processing of EphA4. Neurons were treated with the indicated reagents in the presence or absence of AP5 or CNQX for 16 h. Band intensity was assessed using Photoshop software (Adobe). The intensity of each band of the processed fragment was normalized to control. F, forskolin; R, rolipram; B, bicuculline. Data are expressed as means ± SEM; **, $P < 0.01$; *, $P < 0.05$. (B) Association of EphA4 CTF with the synaptic lipid raft membrane. Neurons were treated with forskolin, rolipram, and bicuculline for 16 h in the presence of compound E, then subjected to sucrose density gradient centrifugation. Equal amounts of the individual fractions were subjected to SDS-PAGE, followed by Western blotting using the indicated antibodies.

Effect of EphA4 ICD on the formation of dendritic spines

To investigate the physiological role of the ICD signaling of EphA4, we prepared an EphA4 ICD mutant encoding the cytoplasmic region of EphA4 and examined its effect on the morphology of dendritic spines. In rat hippocampal primary cultured neurons, HA-EphA4 ICD was diffusely distributed in the somatodendrites, including the nuclei and dendritic spines, which were visualized by TO-PRO-3 and GFP, respectively (Fig. 6 A). Quantitative analysis demonstrated that the number of protrusions increased (control vs. EphA4 ICD: 5.72 ± 0.25 vs. 7.18 ± 0.33 protrusions/10 µm dendrite; $P < 0.01$; Fig. 6 B). However, the mean length and width of the spines were not affected (Fig. 6 B).

Next, we examined whether EphA4 ICD could suppress the compound E–induced inhibitory effect on the formation of dendritic spines. Rat hippocampal primary cultured neurons were transfected with EphA4 ICD and GFP, and then treated with compound E from DIV 14 to 21. Quantitative analysis revealed that treatment with compound E did not reduce the number of dendritic spines in EphA4 ICD–expressing neurons (Fig. 6 C). Furthermore, the number of GluR1 clusters was also not affected (Fig. 6 D). These results suggest that the processing of EphA4 by γ-secretase has a critical role in the formation of dendritic spines, and that EphA4 is one of the critical substrates of γ-secretase that regulates the morphogenesis of dendritic spines.

To confirm these conclusions, we examined the effect of compound E in EphA4 knockdown neurons. We prepared an RNAi construct against EphA4 and confirmed that the RNAi construct specifically reduced the expression of EphA4 (Fig. 7 A). Rat hippocampal primary cultured neurons were transfected with the EphA4 RNAi and analyzed. The number

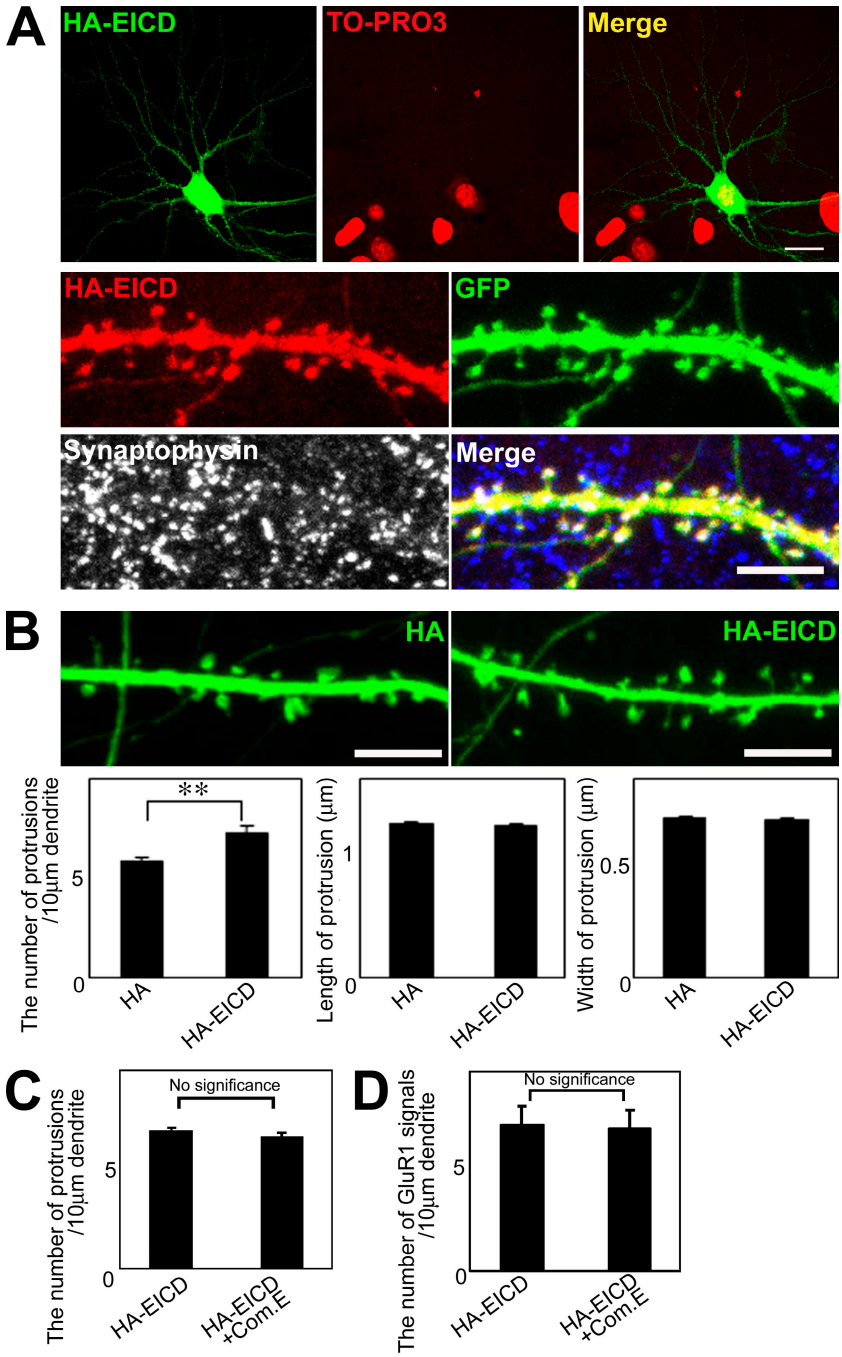

Figure 6. **Effect of EphA4 ICD on spine morphology.** (A) Localization of EphA4 ICD in rat hippocampal primary cultured neurons. Neurons were transfected with HA-EphA4 ICD at DIV 9, then stained with the indicated antibodies at DIV 21. EICD, EphA4 ICD. Bars: (top) 20 μm; (bottom), 5 μm. (B) Effect of EphA4 ICD on spine morphology. Neurons were cotransfected with HA-EphA4 ICD and GFP at DIV 9, then stained with the anti-GFP antibody at DIV 21. Bars, 5 μm. (C) Suppression of the compound E–induced inhibitory effect on the formation of dendritic spines by EphA4 ICD. Neurons were cotransfected with HA-EphA4 ICD and GFP at DIV 9, then treated with DMSO or compound E at DIV 14. The neurons were further incubated for 1 wk and stained with the anti-GFP antibody. (D) Suppression of the compound E–induced inhibitory effect on the clustering of GluR1 by EphA4 ICD. Neurons were cotransfected with HA-EphA4 ICD and GFP at DIV 9, then treated with DMSO or compound E at DIV 14. The neurons were further incubated for 1 wk and stained with the anti-GluR1 antibody. The results represent three independent experiments. Data are expressed as means ± SEM; **, $P < 0.01$.

of dendritic spines was decreased by ~30% compared with control neurons (control vs. EphA4 knockdown: 5.71 ± 0.38 vs. 3.44 ± 0.23 protrusions/10 μm dendrite; $P < 0.01$; Fig. 7 B). In particular, the number of mushroom-type spines, which are known to be functionally mature spines (Matsuzaki et al., 2001), was markedly reduced by ~50% (control vs. EphA4 knockdown: 2.26 ± 0.36 vs. 1.05 ± 0.34 protrusions/10 μm dendrite; $P < 0.05$; Fig. 7 C). We then examined the effect of compound E in EphA4 knockdown neurons. Compound E did not reduce the number of dendritic spines or mushroom-type spines in EphA4 knockdown neurons (Fig. 7, B and C). These results support the notion that EphA4 is one of the critical substrates of γ-secretase that regulates the morphogenesis of dendritic spines.

Molecular mechanism of the action of EphA4 ICD in the morphogenesis of dendritic spines

EphA4 is known to be involved in the signaling pathways of the Rho family proteins (Aoto and Chen, 2007), which are known to regulate reorganization of the actin cytoskeleton. The Rho family consists of three major subfamilies—Cdc42, Rac, and Rho—which are expressed in the brain and involved in the morphogenesis of dendritic spines (Ramakers 2002). To investigate the role of EphA4 ICD in the Rho signaling pathway, the effect of EphA4 ICD on the actin cytoskeleton in NIH3T3 cells was examined. NIH3T3 cells were transfected with HA-EphA4 ICD, and the reorganization of the actin cytoskeleton was analyzed. Immunofluorescence analysis

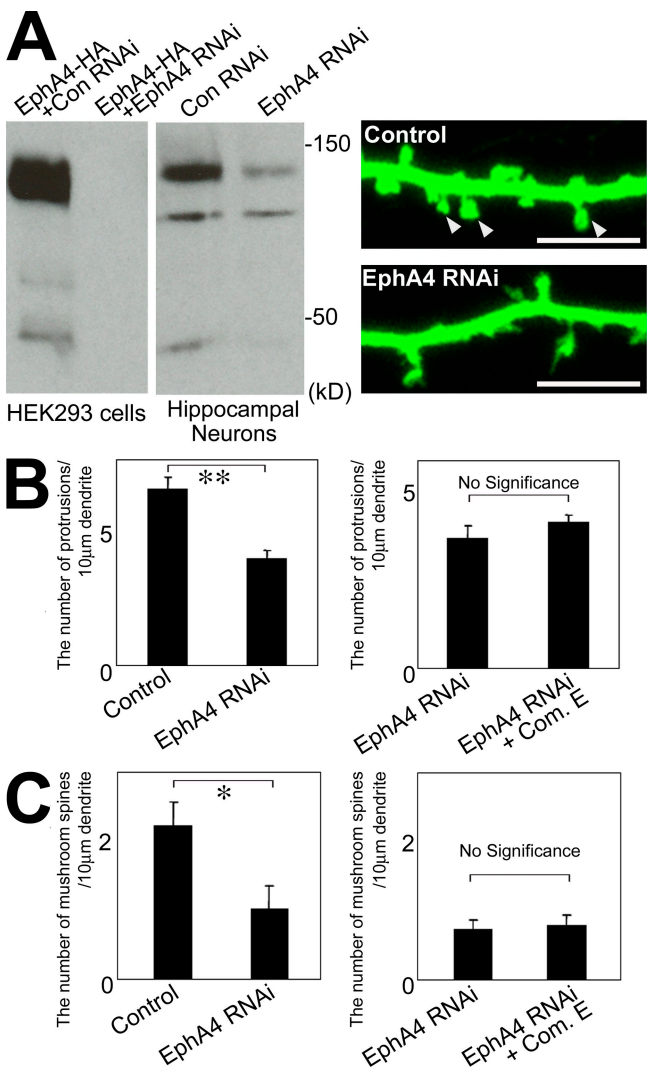

Figure 7. **Effect of γ-secretase inhibitor in EphA4 knockdown neurons.** (A) Effect of EphA4 knockdown on the morphology of dendritic spines. (A, left) Effect of EphA4 RNAi on the expression of EphA4. HEK293 cells were cotransfected with EphA4-HA and the EphA4 RNAi construct. The cell lysate was analyzed by Western blotting. Neurons were electroporated with the EphA4 RNAi construct at DIV 0 and further incubated for 2 wk. The lysate was analyzed by Western blotting. (A, right) Effect of EphA4 knockdown on the morphology of dendritic spines. Neurons were cotransfected with EphA4 RNAi and GFP at DIV 10, and analyzed at DIV 17. Arrowheads indicate mushroom-type spines. Bars, 5 μm. (B) Quantitative analysis of the effect of compound E on the formation of dendritic spines in EphA4 knockdown neurons. The number of total dendritic spines in EphA4 knockdown or compound E–treated EphA4 knockdown neurons was quantified. (C) Quantitative analysis of the effect of compound E on the formation of mushroom-type dendritic spines in EphA4 knockdown neurons. The number of mushroom-type dendritic spines in EphA4 knockdown or compound E–treated EphA4 knockdown neurons was quantified. The results represent three independent experiments. Data are expressed as means ± SEM; **, $P < 0.01$; *, $P < 0.05$.

revealed that HA-EphA4 ICD was distributed in the membrane, cytosol, and nucleus in NIH3T3 cells, and induced the formation of lamellipodia-like structures, which are known to be formed by the activation of Rac (Machesky and Hall, 1997; Fig. 8 A). We next examined which Rho family protein was activated by EphA4 ICD. To analyze the activities, we performed pull-down assays for Rac1, Cdc42, and RhoA. Consistent with the cell biological data, Rac1, but not Cdc42 or RhoA, was activated by EphA4 ICD (Fig. 8 B). These results indicate that EphA4 ICD induces activation of the Rac signaling pathway.

We examined the effects of full-length EphA4, its CTF, an MMP-cleaved membrane-bound precursor of ICD, and ICD on the formation of lamellipodia (Fig. 8 C, left). For preparation of the CTF, the MMP cleavage site of EphA4 was determined by mass spectrometric analysis (unpublished data). We checked the expression levels of these mutants by Western blotting and confirmed that the mutant proteins were expressed in NIH3T3 cells at similar levels (unpublished data). However, the amount of ICD derived from full-length EphA4 was much lower than that of ICD expressed alone (Fig. S2). Consistent with these results, full-length EphA4 did not show the ability to induce lamellipodia, whereas EphA4 ICD enhanced the formation of lamellipodia (Fig. 8 C, right). EphA4 CTF, a precursor of EphA4 ICD, is rapidly cleaved by γ-secretase, resulting in the production of EphA4 ICD (unpublished data). Consistent with this, EphA4 CTF enhanced the formation of lamellipodia (Fig. 8 C, right). Furthermore, the activity of EphA4 CTF was completely abolished after treatment with compound E, whereas the activity of EphA4 ICD was not affected (Fig. 8 C, right), which indicates that EphA4 CTF induces activation of the Rac signaling pathway through the production of EphA4 ICD. Collectively, these results indicate that the processing of EphA4 induces activation of the Rac signaling pathway. Rac is an important regulator for the morphogenesis of dendritic spines, and specifically induces the formation of dendritic spines (Tashiro and Yuste, 2004). Therefore, it is likely that the EphA4 ICD-induced enhancement of the formation of dendritic spines is mediated by activation of the Rac signaling pathway.

To confirm this conclusion, we examined the effect of $Rac1^{N17}$, a dominant-negative mutant, on the EphA4 ICD-induced enhancement of the formation of dendritic spines. To verify that EphA4 ICD activates the Rac signaling pathway, NIH3T3 cells were transfected with HA-EphA4 ICD and $Rac1^{N17}$, and the effect on the formation of lamellipodia was analyzed. $Rac1^{N17}$ abolished the EphA4 ICD-induced enhancement of the formation of lamellipodia (Fig. 8 D). We then examined whether $Rac1^{N17}$ abolished the EphA4 ICD-induced enhancement of the formation of dendritic spines. Similar to NIH3T3 cells, the EphA4 ICD-induced enhancement of the formation of dendritic spines was also abolished by $Rac1^{N17}$. These results indicate that the EphA4 ICD-induced enhancement of the formation of dendritic spines is mediated by activation of the Rac signaling pathway.

To analyze the mode of action of EphA4 ICD, we investigated the localization and function of EphA4 ICD. It is known that ICDs from several substrates localize to the nucleus and function as gene transcription regulators (Landman and Kim, 2004). As shown in Figs. 8 A and 9 A, left, EphA4 ICD existed in the nuclei. Therefore, we examined whether the nuclear localization of EphA4 ICD was necessary for activation of the Rac signaling pathway. To address this, we used a myristoylated EphA4 ICD mutant, which is a membrane-anchoring mutant and does not localize to the nucleus. To prepare the mutant construct, we added the myristoylation sequence of c-Src to the N terminus of EphA4 ICD. We then examined the effect of the myristoylated

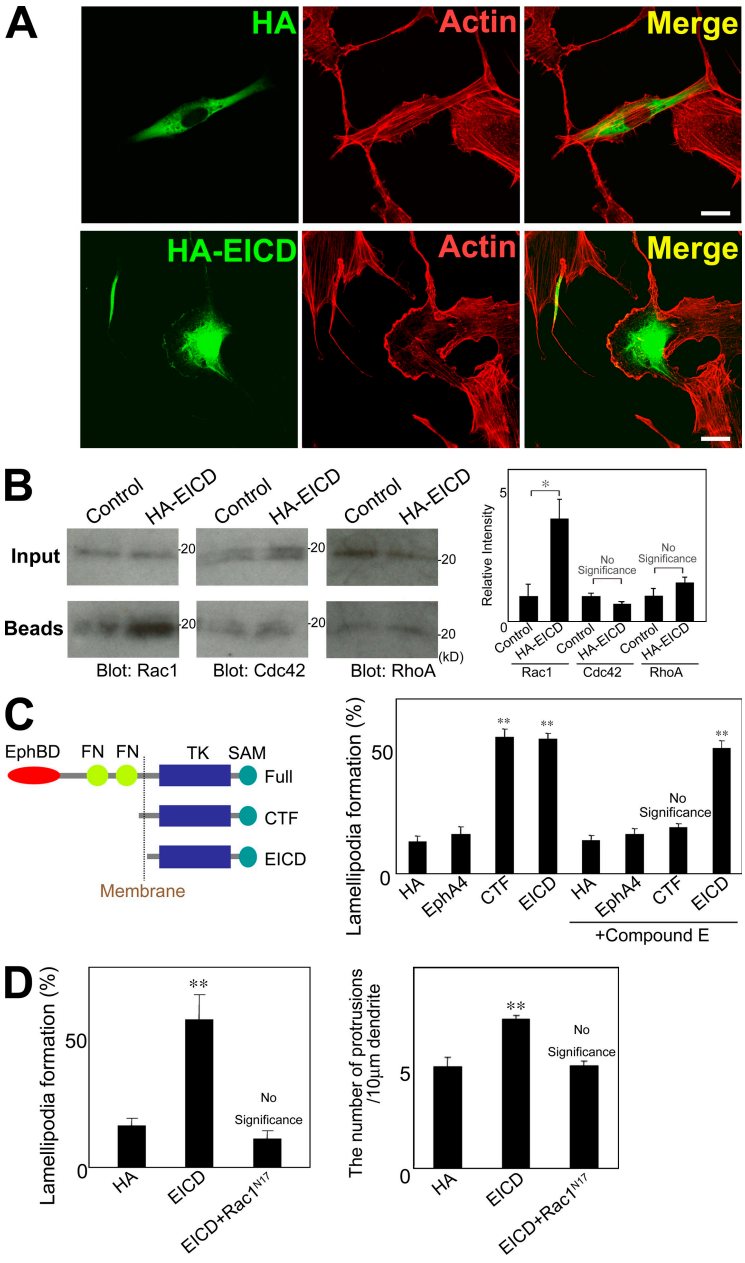

Figure 8. **Activation of Rac by the processing of EphA4.** (A) Effect of EphA4 ICD on reorganization of the actin cytoskeleton in NIH3T3 cells. Cells were transfected with HA or HA-EphA4 ICD, then stained with Alexa Fluor 546–phalloidin and the anti-HA antibody. EICD, EphA4 ICD. Bars, 20 μm. (B) Activation of Rac1 by EphA4 ICD. NIH3T3 cells expressing HA-EphA4 ICD were subjected to a pull-down assay, followed by Western blotting using the anti-Rac1, the anti-Cdc42, and the anti-RhoA antibodies. The intensity of the activity was normalized to control. (C) Effects of various EphA4 mutants on the formation of lamellipodia. (C, left) Various EphA4 constructs. EphBD, Ephrin-binding domain; FN, fibronectin domain; TK, tyrosine kinase domain; SAM, SAM domain. (C, right) Quantification of the formation of lamellipodia-like structures. The efficiencies of lamellipodia formation induced by the indicated constructs were analyzed. (D) Inhibition of the EphA4 ICD-induced effect by $Rac1^{N17}$. (D, left) Inhibition of EphA4 ICD-induced enhancement of the formation of lamellipodia by $Rac1^{N17}$. NIH3T3 cells were cotransfected with HA-EphA4 ICD and $Rac1^{N17}$, then analyzed. (D, right) Inhibition of EphA4 ICD-induced enhancement of the formation of dendritic spines by $Rac1^{N17}$. Neurons were cotransfected with HA-EphA4 ICD and $Rac1^{N17}$, then analyzed. The results represent three independent experiments. Data are expressed as means ± SEM; **, $P < 0.01$; *, $P < 0.05$.

EphA4 ICD mutant on the formation of lamellipodia. Immunofluorescence analysis revealed that the signals for the myristoylated EphA4 ICD mutant exhibited a dot-like pattern and were distributed in the cytosol and membrane, but not in the nucleus (Fig. 9 A, left). Under these conditions, the myristoylated EphA4 ICD mutant significantly enhanced the formation of lamellipodia, whereas the degree was slightly lower than that of EphA4 ICD (Fig. 9 A, right). These results indicate that nuclear localization of EphA4 ICD is not necessary for the activation of the Rac signaling pathway.

The kinase activity of EphA4 is known to be important for the Ephrin-dependent signaling pathway (Aoto and Chen, 2007). Therefore, we examined whether full-length EphA4, its CTF, and ICD were phosphorylated in NIH3T3 cells. Biochemical analysis revealed that all of these proteins were phosphorylated in NIH3T3 cells (Fig. 9 B, left). However, full-length $EphA4^{K653M}$ and EphA4 ICD^{K653M}, which are kinase-dead mutants, was not phosphorylated (Fig. 9 B, left). To investigate the requirement of the kinase activity of EphA4 ICD for the activation of the Rac signaling pathway, we examined the effect of EphA4 ICD^{K653M} on the formation of lamellipodia. EphA4 ICD^{K653M} enhanced the formation of lamellipodia to the same level as EphA4 ICD (Fig. 9 B, right). These results indicate that the kinase activity of EphA4 is not required for EphA4 ICD-induced activation of the Rac signaling pathway.

The effect of familial Alzheimer's disease–linked mutation of PS1 on the processing of EphA4

It has been shown that familial Alzheimer's disease–linked mutations of PS1 impair the processing of several substrates (Bentahir et al., 2006). To examine the effect of familial Alzheimer's

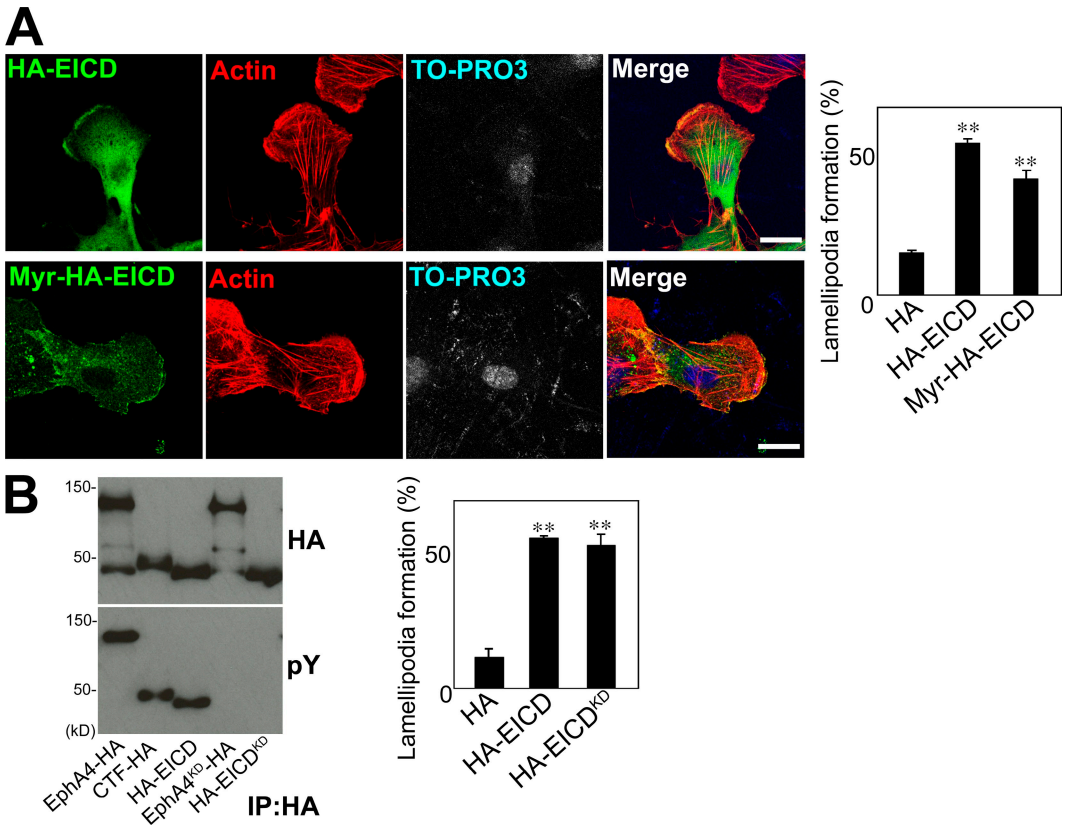

Figure 9. **Mode of action of EphA4 ICD.** (A) Effect of myristoylated EphA4 ICD on the formation of lamellipodia. (A, left) Localizations of EphA4 ICD and myristoylated EphA4 ICD. NIH3T3 cells were transfected with HA-EphA4 ICD or myristoylated HA-EphA4 ICD, and the morphology of the actin cytoskeleton was then analyzed. Bars, 20 µm. (A, right) Quantitative analysis of the effect of myristoylated EphA4 ICD on the formation of lamellipodia. EICD, EphA4 ICD. (B) Requirement of the kinase activity of EphA4 for enhancement of the formation of lamellipodia. (B, left) Phosphorylation of various EphA4 mutants in NIH3T3 cells. NIH3T3 cells were transfected with the indicated mutants, and the mutant proteins were then immunoprecipitated with the anti-HA antibody. The beads were analyzed by Western blotting using the anti-HA and the anti–phospho-tyrosine antibodies. pY, phospho-tyrosine. (B, right) Quantitative analysis of the effect of EphA4 ICD^{K653M} on the formation of lamellipodia. Data are expressed as means ± SEM; **, $P < 0.01$. The results represent three independent experiments.

disease–linked mutation of PS1 on the processing of EphA4, we performed an in vitro γ-secretase assay using membranes from PS double knockout cells expressing intact PS1, dominant-negative PS1 (PS1^{D385A}), and familial Alzheimer's disease–linked PS1 mutants (PS1^{M146L} and PS1^{E280A}). The membranes from PS double knockout cells expressing the PS1 mutants, except for the vector control or PS1^{D385A}, produced EphA4 ICD (Fig. 10 A). However, the amounts of EphA4 ICD generated from the membranes of cells expressing the familial Alzheimer's disease–linked PS mutants were much lower than those from the membranes of cells expressing intact PS1 (Fig. 10 A). These results indicate that the processing of EphA4 is impaired by familial Alzheimer's disease–linked mutations of PS1.

Discussion

Localization and function of γ-secretase

Several studies using cultured neurons or cell lines have demonstrated that γ-secretase is localized within intracellular membranes such as the Golgi apparatus (Annaert et al., 1999; Rechards et al., 2003). In the present study, immunohistochemical and biochemical analyses demonstrated that γ-secretase was localized at synapses and tightly associated with the synaptic lipid raft membrane, although it could not be determined whether γ-secretase was localized at presynapses and/or postsynapses. It has been shown that PS1 is associated with the NMDA receptor (Saura et al., 2004). Consistent with this result, we demonstrated that inactivation of γ-secretase decreased the number of dendritic spines and GluR1 clusters without affecting synaptic vesicle clustering (Fig. 2 A). These findings suggest that γ-secretase localizes and functions at postsynapses.

PS1/PS2 conditional double knockout mice display decreased synaptic activity and age-dependent loss of synapses (Saura et al., 2004). Consistent with these findings, we showed that the number of GluR1 clusters was decreased by a γ-secretase inhibitor, whereas neither synaptophysin nor PSD-95 was affected. It is known that some synapses do not contain AMPA receptors; these synapses are termed silent synapses (Isaac et al., 1995). Recently, overexpression of SynGAP, a synaptic Ras GTPase-activating protein, was found to lead to a reduction of GluR1 clusters without affecting total synapse number, resulting in an increase in silent synapses (Rumbaugh et al., 2006). These findings suggest that active synapses may be decreased by the γ-secretase inhibitor. Indeed, strong GluR1/synaptophysin or strong GluR1/PSD-95 colocalization signals were apparently decreased in the γ-secretase inhibitor–treated neurons (Fig. 2 A).

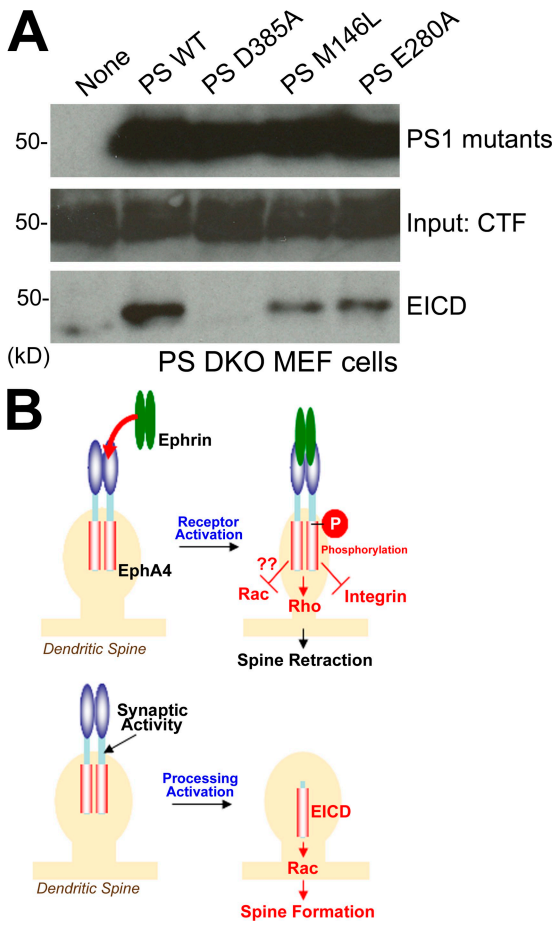

Figure 10. **Schematic diagram of EphA4 signaling at dendritic spines.** (A) Effect of familial Alzheimer's disease–linked mutation of PS1 on the processing of EphA4. PS double knockout cells were cotransfected with EphA4 CTF-HA and the indicated PS1 mutants. The purified membrane fractions were incubated for 4 h. The generated ICD was purified by immunoprecipitation using the anti-HA antibody, followed by Western blotting. (B) Schematic diagram of EphA4 signaling at dendritic spines. (B, top) Ephrin-dependent retraction of dendritic spines. Activation of EphA4 by Ephrin retracts dendritic spines by activating the RhoA signaling pathway, by inhibiting the integrin signaling pathways, and, possibly, by inhibiting the Rac signaling pathway. (B, bottom) γ-secretase–dependent enhancement of the formation of dendritic spines. Activity-induced processing of EphA4 by γ-secretase enhances the formation of dendritic spines by activating the Rac signaling pathway. EICD, EphA4 ICD.

Of note, the size of the clusters of PSD-95 was slightly enlarged by the γ-secretase inhibitor. The molecular mechanism of the phenotype is currently unknown, but it is likely that another γ-secretase substrate that regulates the clustering of PSD-95 may be involved. Indeed, the well-known γ-secretase substrate ErbB4 is associated with PSD-95 at synapses (Garcia et al., 2000). Not only EphA4 but also other γ-secretase substrates may regulate the development of postsynapses.

In the present study, we showed that the number of dendritic spines was reduced by inactivation of γ-secretase. It has been shown that the morphology of dendritic spines is correlated to the strength of synaptic activity, especially AMPA receptor function (Matsuzaki et al., 2001). These findings are consistent with the abnormal localization of GluR1 in γ-secretase inhibitor–treated neurons. We found that the processing of EphA4 by γ-secretase activated the Rac signaling pathway, which is a master regulator for the actin cytoskeleton in dendritic spines (Ramakers 2002; Tashiro and Yuste, 2004). Down-regulation of the Rac signaling pathway was also found to result in a reduction of the clustering of the AMPA receptor (Xie et al., 2007). These findings imply that γ-secretase is involved in functional and structural maturation of dendritic spines through regulation of the Rac signaling pathway.

Regulation of EphA4 signaling by γ-secretase

Inactivation of γ-secretase by conditional PS1/PS2 double knockout impairs long-term potentiation (Saura et al., 2004). Long-term potentiation induces rapid enlargement of dendritic spines, resulting in enhanced synaptic transmission (Kopec et al., 2006). These observations suggest that γ-secretase plays a role in the synaptic activity-dependent morphogenesis of dendritic spines. The present study demonstrated that the processing of EphA4 was enhanced by synaptic activity. Furthermore, EphA4 ICD expression enhanced the formation of dendritic spines. These results suggest that the processing of EphA4 is regulated by synaptic activity and at least partly involved in the synaptic activity–dependent morphological changes of dendritic spines.

ICDs from several γ-secretase substrates, such as Notch, localize to the nucleus and regulate gene transcription (Landman and Kim, 2004). EphA4 ICD was found to exist in the nuclei. However, a myristoylated EphA4 ICD mutant, which did not localize to the nucleus, had almost the same activity as intact EphA4 ICD in the Rac signaling pathway. The result indicates that the nuclear localization of EphA4 ICD is not required for the activation of the Rac signaling pathway, and suggests that a downstream molecule for EphA4 ICD is localized near the membrane. EphA4 ICD has various signaling domains, such as a kinase domain and a PDZ-binding motif. In the present study, we revealed that the kinase activity of EphA4 ICD was not necessary for the activation of the Rac signaling pathway. Furthermore, the PDZ-binding motif was not required (Fig. S2). These results indicate that EphA4 ICD does not activate the Rac signaling pathway through the kinase-mediated signaling or regulation of PDZ proteins. Synaptic activity activates various Rac modulators, such as Tiam1, Kalirin-7, and βPIX, and enhances the formation of dendritic spines through the activation of the Rac signaling pathway (Penzes et al., 2008). These findings lead us to speculate that the processing of EphA4 may be involved in the signaling pathways of these modulators. Identification of the target molecules for EphA4 ICD is necessary to understand the molecular mechanism of the action of EphA4 ICD.

Activation of EphA4 by Ephrin is known to result in retracted dendritic spines (Murai et al., 2003), which is reported to be mediated by the activation of RhoA and the inhibition of integrin pathways (Bourgin et al., 2007; Fu et al., 2007). In addition, an EphA4-associated Rac GTPase-activating protein, α-chimerin, which is activated by Ephrin (Iwasato et al., 2007), was found to be involved in the retraction of dendritic spines (Fig. 10 B, top; Van de Ven et al., 2005). The present study demonstrated that the processing of EphA4 by γ-secretase enhanced the formation of dendritic spines through the activation of the Rac signaling pathway,

in contrast to the EphrinA-dependent signaling (Fig. 10 B, bottom). Indeed, the processing of EphA4 was not dependent on EphrinA stimulation and promoted the formation of dendritic spines. These results suggest that EphA4 has a dual function in the morphogenesis of dendritic spines (Fig. 10 B). Studies have shown that temporal and spatial regulations of Rho and Rac activities are crucial for the maintenance of dendritic spines (Elia et al., 2006). Therefore, the regulation of EphA4 signaling by Ephrin and γ-secretase is thought to have a critical role in the morphogenesis of dendritic spines (Fig. 10 B).

Possible role of γ-secretase in Alzheimer's disease pathogenesis

In this paper, we show that the processing of EphA4 was impaired by familial Alzheimer's disease–linked mutations of PS. These findings suggest that failure of the processing of EphA4 is involved in the pathogenesis of Alzheimer's disease. As described above, we demonstrated that the processing of EphA4 activates the Rac signaling pathway (Fig. 8). Recently, PAK, a downstream target of Rac, was reported to be down-regulated in the Alzheimer's disease brain (Zhao et al., 2006). These findings suggest that the Rac–PAK signaling pathway has a critical role in the pathogenesis of Alzheimer's disease, and that the processing of EphA4 may be involved in this pathogenesis.

Collectively, γ-secretase plays a critical role in the formation of dendritic spines, and γ-secretase inactivation leads to impaired formation and maintenance of dendritic spines. At synapses, γ-secretase processes EphA4 to generate ICD, which is capable of promoting the formation of dendritic spines through the activation of the Rac signaling pathway. This processing is regulated by synaptic activity. Therefore, it is likely that the processing of EphA4 has a role in the synaptic activity–dependent morphogenesis of dendritic spines.

Materials and methods

Antibodies

A rabbit antiserum was raised against GST-PS1 (aa 1–80) and affinity-purified as described previously (Inoue et al., 2006). The following antibodies were used: rabbit polyclonal anti-EphA4 (Millipore), rabbit polyclonal anti-GluR1 (Millipore), rabbit polyclonal anti–phospho-GluR1 Ser845 (Millipore), rabbit polyclonal anti-Nicastrin (Sigma-Aldrich), rabbit polyclonal anti-PS1 (Sigma-Aldrich), rabbit polyclonal anti-PS2 (EMD), mouse monoclonal anti-Bassoon (Assay Designs), mouse monoclonal anti-PSD-95 (Thermo Fisher Scientific), mouse monoclonal anti-synaptophysin (Millipore), mouse monoclonal anti–Flotillin-1 (BD), mouse monoclonal anti-NMDA receptor 1 (BD), mouse monoclonal anti-Rac1 (Thermo Fisher Scientific), mouse monoclonal anti-Cdc42 (BD), mouse monoclonal anti-RhoA (Santa Cruz Biotechnology, Inc.), mouse monoclonal phospho-tyrosine (pY20; Santa Cruz Biotechnology, Inc.), rat polyclonal anti-Homer (Abcam), rabbit polyclonal anti-GFP (Invitrogen), and rat monoclonal anti-HA (3F10; Roche).

Cell culture

Rat primary cultured hippocampal neurons were prepared from embryonic day 18 rats as described previously (Inoue et al., 2006). The γ-secretase inhibitor compound E (50 nM; Enzo Biochem, Inc.) was applied to culture medium at DIV 14, and the treated neurons were analyzed at DIV 21. To stimulate MMP activity, neurons were incubated in 10 µM ionomycin (Sigma-Aldrich) in the presence or absence of 2.5 µM GM6001 (EMD) for 30 min. For treatment with the EphrinA3-Fc fusion protein, neurons at DIV 21 were treated with EphrinA3-Fc (10 µg/ml; R&D Systems) in the presence of 50 nM of compound E for 2 h. To stimulate synaptic activity, neurons at DIV 21 were incubated in 50 µM forskolin (Sigma-Aldrich), 0.1 µM rolipram (Sigma-Aldrich), and 50 µM bicuculline (Sigma-Aldrich) for 16 h. For morphological analysis, neurons were maintained in Neurobasal medium (Invitrogen) supplemented with B27/0.5 mM glutamine, and transfected at DIV 9–17 using Lipofectamine 2000 (Invitrogen) as described previously (Hoogenraad et al., 2007). Subsequently, the cells were fixed and analyzed by immunocytochemistry at DIV 17–22. PS1/PS2 double knockout cells were obtained from B. De Strooper (Center for Human Genetics, Katholieke Universiteit Leuven, Belgium). HEK293, PS1/PS2 double knockout, and NIH3T3 cells were maintained in DME (Invitrogen) supplemented with 10% fetal calf serum or calf bovine serum. Retroviruses were prepared with a retrovirus packaging kit (Takara Bio, Inc.), according to the manufacturer's instructions. For analysis of the processing of exogenous EphA4, HEK293 cells were transfected with EphA4-HA using Lipofectamine 2000 and incubated for 1 d. The cells were then treated with 50 nM of compound E and further incubated for 1 d. For analysis using PS double knockout cells, cells were transfected with EphA4-HA and incubated for 1 d. After the incubation, the cells were analyzed by Western blotting.

In vitro γ-secretase assay

HEK293 cells expressing EphA4-HA were harvested with A buffer (50 mM Pipes, pH 7.0, 5 mM $MgCl_2$, 5 mM $CaCl_2$, and 150 mM KCl). After 12 passages through a 26-gauge needle, the homogenates were fractionated by centrifugation at 800 *g* for 10 min. The supernatants were further centrifuged at 48,200 *g* for 20 min. The pellet fractions were resuspended with A buffer and incubated at 37°C for 16 h in the presence or absence of 50 nM of compound E. After centrifugation, EphA4 ICD was purified from the supernatant using the anti-HA antibody. For analyses of familial Alzheimer's disease–linked PS1 mutants, PS double knockout cells were cotransfected with CTF-HA and each mouse PS1 mutant. After 1 d, the cells were harvested with A buffer. The purified membrane fractions were incubated at 37°C for 4 h. After centrifugation, EphA4 ICD was purified from the supernatants using the anti-HA antibody.

Immunocytochemistry

Cells were fixed with 2% paraformaldehyde/4% sucrose in PBS, pH 7.4, at room temperature for 20 min, or with methanol at −20°C for 20 min. After PBS washing steps, cells were permeabilized with 0.25% Triton X-100/PBS for 15 min. Nonspecific binding was blocked for 1 h with 4% Block Ace (Dainippon Pharmaceutical) containing 0.25% Triton X-100 or OptiMEM (Invitrogen) containing 2% BSA and 0.25% Triton X-100. The cells were incubated with primary antibodies for 1 h, followed by secondary antibodies. The stained cells were analyzed by confocal laser microscopy (LSM510; Carl Zeiss, Inc.) using a 100× oil immersion objective lens (Carl Zeiss, Inc.). For quantitative analyses, acquired images were analyzed using MetaMorph software (MDS Analytical Technologies).

Immunohistochemistry

Immunohistochemistry of mouse hippocampal tissues was performed as described previously (Inoue et al., 2006). In brief, adult mice were deeply anesthetized and perfused with freshly prepared 2% paraformaldehyde/phosphate buffer for 10 min. Brains were resected and sectioned into several 1-mm-thick coronal pieces, which were soaked in the same fixative for 2 h at 4°C. For cryoprotection, the tissue pieces were placed into 20% sucrose solution for 4 h and 25% sucrose solution overnight, then frozen using liquid nitrogen. Serial 10-µm-thick sections were cut using a cryostat (Leica). The sections were blocked with 1% BSA/10% normal donkey serum/0.5% Triton X-100 in PBS for 20 min, followed by incubation with primary antibodies. The sections were then washed and incubated with secondary antibodies. The sections were subsequently washed with PBS, embedded, and analyzed by confocal laser microscopy (LSM510) using a 100× oil immersion objective lens.

cDNA cloning and expression vectors

Rat EphA4, PS1, PS2, mouse PS1, and PS2 were PCR-amplified from rat or mouse brain first-strand cDNAs, which were prepared with an RNA PCR kit (Takara Bio, Inc.). The cDNA fragments were subcloned into pBluescript (Agilent Technologies), and the cloned cDNA sequences were confirmed using a DNA sequencer (Applied Biosystems). Expression vectors were constructed in pCAG-HA (Niwa et al., 1991) using standard molecular biological methods. EphA4 constructs were created for the following aa residues: EphA4 (aa 1-stop), CTF (aa 530-stop), and ICD (aa 571-stop). The following RNAi constructs against rat PS1, PS2, and EphA4 were cloned into pSilencer (Applied Biosystems): PS1, 5′-ACAGTGTTCTGGTTGGTAA-3′; PS2, 5′-GGTCATGACTATCTTCCTA-3′; and EphA4, 5′-GCAATTGCGTATCGTAAAT-3′. Mouse $PS1^{D385A}$, $PS1^{M146L}$, $PS1^{E280A}$, and rat $EphA4^{K653M}$ were generated by site-directed mutagenesis using a GeneTailor Site-Directed Mutagenesis System (Invitrogen) according to the manufacturer's

instructions. For myristoylated EphA4 ICD, the myristoylation sequence (MGSSKSKPK) of c-Src was fused to the N terminus of HA-EphA4 ICD.

Biochemical analysis

Subcellular fractionation of the rat brain was performed as described previously (Inoue et al., 2006). To obtain the lipid raft membrane fraction, sucrose density fractionation was performed as described previously (Vetrivel et al., 2004), with slight modifications. In brief, the crude synaptic membrane fraction was suspended with 0.5% Lubrol/TNE (20 mM Tris-HCl, pH 7.4, 150 mM NaCl, and 1mM EDTA). After 12 passages through a 26-gauge needle, the sample was mixed at 4°C for 30 min. The lysate was adjusted to a final concentration of 40% sucrose. A discontinuous sucrose gradient was then prepared by sequentially layering 30%, 25%, and 5% sucrose. The tubes were subjected to ultracentrifugation at 201,800 *g* for 2 h. 11 fractions (1 ml each), as well as the bottom fraction, were collected from the top of the gradient. Equal volumes of the fractions were analyzed by Western blotting. For substrate identification, a 10-µg sample of the purified synaptic lipid raft membrane fraction was subjected to SDS-PAGE, followed by Coomassie Brilliant blue staining (Bio-Rad Laboratories). Sample preparation and protein identification were performed by mass spectrometric analysis as described previously (Tabata et al., 2007), with the exception that data were analyzed by Mascot (Matrix Science). For neuronal sucrose density fractionation, rat hippocampal primary cultured neurons at DIV 21–22 were washed with PBS, followed by 0.5% Lubrol/TNE extraction. Density gradient fractionation was performed in the same way as with the purification of lipid raft membrane from the crude synaptic membrane fraction.

Rac pull-down assay

NIH3T3 cells were infected with a retrovirus expressing HA-EphA4 ICD. The cells were then washed with ice-cold PBS, and lysed in a lysis buffer (50 mM Tris-HCl, pH 7.4, 150 mM NaCl, 5 mM $MgCl_2$, 1% NP-40, 0.5% sodium deoxycholate, and 0.1% SDS). The cell lysates were incubated with GST-p21–binding domain beads for Rac1 and Cdc42, or GST-Rho–binding domain beads for RhoA (Cytoskeleton, Inc.) at 4°C for 1 h. After washing the beads with the lysis buffer, the bound proteins were analyzed by Western blotting. Band intensity was assessed using Photoshop software (Adobe). The band intensities of GTP-Rho family proteins were quantified as a ratio of the total protein and then normalized to control.

Online supplemental material

Fig. S1 shows the specificity of PS double knockdown. Fig. S2 shows the analysis of the effect of various EphA4 mutants on the formation of lamellipodia in NIH3T3 cells. Online supplemental material is available at http://www.jcb.org/cgi/content/full/jcb.200809151/DC1.

We would like to thank Dr. B. De Strooper for the PS double knockout mouse embryonic fibroblast cells.

Submitted: 22 September 2008
Accepted: 8 April 2009

References

Annaert, W.G., L. Levesque, K. Craessaerts, I. Dierinck, G. Snellings, D. Westaway, P. St. George-Hyslop, B. Cordell, P. Fraser, and B. De Strooper. 1999. Presenilin 1 controls γ-secretase processing of the amyloid precursor protein in pre-Golgi compartments of hippocampal neurons. *J. Cell Biol.* 147:277–294.

Aoto, J., and L. Chen. 2007. Bidirectional ephrin/Eph signaling in synaptic functions. *Brain Res.* 1184:72–80.

Arriagada, P.V., K. Marzloff, and B.T. Hyman. 1992. Distribution of Alzheimer-type pathologic changes in nondemented elderly individuals matches the pattern in Alzheimer's disease. *Neurology.* 42:1681–1688.

Beher, D., C. Elle, J. Underwood, J.B. Davis, R. Ward, E. Karran, C.L. Masters, K. Beyreuther, and G. Multhaup. 1999. Proteolytic fragments of Alzheimer's disease-associated presenilin 1 are present in synaptic organelles and growth cone membranes of rat brain. *J. Neurochem.* 72:1564–1573.

Bentahir, M., O. Nyabi, J. Verhamme, A. Tolia, K. Horré, J. Wiltfang, H. Esselmann, and B. De Strooper. 2006. Presenilin clinical mutations can affect γ-secretase activity by different mechanisms. *J. Neurochem.* 96:732–742.

Bickel, P.E., P.E. Scherer, J.E. Schnitzer, P. Oh, M.P. Lisanti, and H.F. Lodish. 1997. Flotillin and epidermal surface antigen define a new family of caveolae-associated integral membrane proteins. *J. Biol. Chem.* 272:13793–13802.

Bourgin, C., K.K. Murai, M. Richter, and E.B. Pasquale. 2007. The EphA4 receptor regulates dendritic spine remodeling by affecting β1-integrin signaling pathways. *J. Cell Biol.* 178:1295–1307.

Derkach, V.A., M.C. Oh, E.S. Guire, and T.R. Soderling. 2007. Regulatory mechanisms of AMPA receptors in synaptic plasticity. *Nat. Rev. Neurosci.* 8:101–113.

De Strooper, B. 2003. Aph-1, Pen-2, and Nicastrin with Presenilin generate an active γ-secretase complex. *Neuron.* 38:9–12.

Elia, L.P., M. Yamamoto, K. Zang, and L.F. Reichardt. 2006. p120 catenin regulates dendritic spine and synapse development through Rho-family GTPases and cadherins. *Neuron.* 51:43–56.

Fu, W.Y., Y. Chen, M. Sahin, X.S. Zhao, L. Shi, J.B. Bikoff, K.O. Lai, W.H. Yung, A.K. Fu, M.E. Greenberg, and N.Y. Ip. 2007. Cdk5 regulates EphA4-mediated dendritic spine retraction through an ephexin1-dependent mechanism. *Nat. Neurosci.* 10:67–76.

Garcia, R.A., K. Vasudevan, and A. Buonanno. 2000. The neuregulin receptor ErbB-4 interacts with PDZ-containing proteins at neuronal synapses. *Proc. Natl. Acad. Sci. USA.* 97:3596–3601.

Georgakopoulos, A., C. Litterst, E. Ghersi, L. Baki, C. Xu, G. Serban, and N.K. Robakis. 2006. Metalloproteinase/Presenilin1 processing of ephrinB regulates EphB-induced Src phosphorylation and signaling. *EMBO J.* 25:1242–1252.

Haapasalo, A., D.Y. Kim, B.W. Carey, M.K. Turunen, W.H. Pettingell, and D.M. Kovacs. 2007. Presenilin/γ-secretase-mediated cleavage regulates association of leukocyte-common antigen-related (LAR) receptor tyrosine phosphatase with β-catenin. *J. Biol. Chem.* 282:9063–9072.

Hering, H., C.C. Lin, and M. Sheng. 2003. Lipid rafts in the maintenance of synapses, dendritic spines, and surface AMPA receptor stability. *J. Neurosci.* 23:3262–3271.

Herreman, A., D. Hartmann, W. Annaert, P. Saftig, K. Craessaerts, L. Serneels, L. Umans, V. Schrijvers, F. Checler, H. Vanderstichele, et al. 1999. Presenilin 2 deficiency causes a mild pulmonary phenotype and no changes in amyloid precursor protein processing but enhances the embryonic lethal phenotype of presenilin 1 deficiency. *Proc. Natl. Acad. Sci. USA.* 96:11872–11877.

Herreman, A., G. Van Gassen, M. Bentahir, O. Nyabi, K. Craessaerts, U. Mueller, W. Annaert, and B. De Strooper. 2003. γ-secretase activity requires the presenilin-dependent trafficking of nicastrin through the Golgi apparatus but not its complex glycosylation. *J. Cell Sci.* 116:1127–1136.

Hoogenraad, C.C., M.I. Feliu-Mojer, S.A. Spangler, A.D. Milstein, A.W. Dunah, A.Y. Hung, and M. Sheng. 2007. Liprin α1 degradation by calcium/calmodulin-dependent protein kinase II regulates LAR receptor tyrosine phosphatase distribution and dendrite development. *Dev. Cell.* 12:587–602.

Inoue, E., S. Mochida, H. Takagi, S. Higa, M. Deguchi-Tawarada, E. Takao-Rikitsu, M. Inoue, I. Yao, K. Takeuchi, I. Kitajima, et al. 2006. SAD: a presynaptic kinase associated with synaptic vesicles and the active zone cytomatrix that regulates neurotransmitter release. *Neuron.* 50:261–275.

Isaac, J.T., R.A. Nicoll, and R.C. Malenka. 1995. Evidence for silent synapses: implications for the expression of LTP. *Neuron.* 15:427–434.

Iwasato, T., H. Katoh, H. Nishimaru, Y. Ishikawa, H. Inoue, Y.M. Saito, R. Ando, M. Iwama, R. Takahashi, M. Negishi, and S. Itohara. 2007. Rac-GAP α-chimerin regulates motor-circuit formation as a key mediator of EphrinB3/EphA4 forward signaling. *Cell.* 130:742–753.

Kamal, A., A. Almenar-Queralt, J.F. LeBlanc, E.A. Roberts, and L.S. Goldstein. 2001. Kinesin-mediated axonal transport of a membrane compartment containing β-secretase and presenilin-1 requires APP. *Nature.* 414:643–648.

Kazee, A.M., and E.M. Johnson. 1998. Alzheimer's disease pathology in nondemented elderly. *J. Alzheimers Dis.* 1:81–89.

Kim, E., and M. Sheng. 2004. PDZ domain proteins of synapses. *Nat. Rev. Neurosci.* 5:771–781.

Kopec, C.D., B. Li, W. Wei, J. Boehm, and R. Malinow. 2006. Glutamate receptor exocytosis and spine enlargement during chemically induced long-term potentiation. *J. Neurosci.* 26:2000–2009.

Landman, N., and T.W. Kim. 2004. Got RIP? Presenilin-dependent intramembrane proteolysis in growth factor receptor signaling. *Cytokine Growth Factor Rev.* 15:337–351.

Le Borgne, R., A. Bardin, and F. Schweisguth. 2005. The roles of receptor and ligand endocytosis in regulating Notch signaling. *Development.* 132:1751–1762.

Litterst, C., A. Georgakopoulos, J. Shioi, E. Ghersi, T. Wisniewski, R. Wang, A. Ludwig, and N.K. Robakis. 2007. Ligand binding and calcium influx induce distinct ectodomain/γ-secretase-processing pathways of EphB2 receptor. *J. Biol. Chem.* 282:16155–16163.

Machesky, L.M., and A. Hall. 1997. Role of actin polymerization and adhesion to extracellular matrix in Rac- and Rho-induced cytoskeletal reorganization. *J. Cell Biol.* 138:913–926.

Marambaud, P., P.H. Wen, A. Dutt, J. Shioi, A. Takashima, R. Siman, and N.K. Robakis. 2003. A CBP binding transcriptional repressor produced by the PS1/ε-cleavage of N-cadherin is inhibited by PS1 FAD mutations. *Cell.* 114:635–645.

Maretzky, T., M. Schulte, A. Ludwig, S. Rose-John, C. Blobel, D. Hartmann, P. Altevogt, P. Saftig, and K. Reiss. 2005. L1 is sequentially processed

by two differently activated metalloproteases and presenilin/γ-secretase and regulates neural cell adhesion, cell migration, and neurite outgrowth. *Mol. Cell. Biol.* 25:9040–9053.

Matsuzaki, M., G.C. Ellis-Davies, T. Nemoto, Y. Miyashita, M. Iino, and H. Kasai. 2001. Dendritic spine geometry is critical for AMPA receptor expression in hippocampal CA1 pyramidal neurons. *Nat. Neurosci.* 4:1086–1092.

Moehlmann, T., E. Winkler, X. Xia, D. Edbauer, J. Murrell, A. Capell, C. Kaether, H. Zheng, B. Ghetti, C. Haass, and H. Steiner. 2002. Presenilin-1 mutations of leucine 166 equally affect the generation of the Notch and APP intracellular domains independent of their effect on Aβ 42 production. *Proc. Natl. Acad. Sci. USA.* 99:8025–8030.

Murai, K.K., L.N. Nguyen, F. Irie, Y. Yamaguchi, and E.B. Pasquale. 2003. Control of hippocampal dendritic spine morphology through ephrin-A3/EphA4 signaling. *Nat. Neurosci.* 6:153–160.

Niwa, H., K. Yamamura, and J. Miyazaki. 1991. Efficient selection for high-expression transfectants with a novel eukaryotic vector. *Gene.* 108:193–199.

Oh, M.C., V.A. Derkach, E.S. Guire, and T.R. Soderling. 2006. Extrasynaptic membrane trafficking regulated by GluR1 serine 845 phosphorylation primes AMPA receptors for long-term potentiation. *J. Biol. Chem.* 281:752–758.

Otmakhov, N., L. Khibnik, N. Otmakhova, S. Carpenter, S. Riahi, B. Asrican, and J. Lisman. 2004. Forskolin-induced LTP in the CA1 hippocampal region is NMDA receptor dependent. *J. Neurophysiol.* 91:1955–1962.

Penzes, P., M.E. Cahill, K.A. Jones, and D.P. Srivastava. 2008. Convergent CaMK and RacGEF signals control dendritic structure and function. *Trends Cell Biol.* 18:405–413.

Ramakers, G.J. 2002. Rho proteins, mental retardation and the cellular basis of cognition. *Trends Neurosci.* 25:191–199.

Rechards, M., W. Xia, V.M. Oorschot, D.J. Selkoe, and J. Klumperman. 2003. Presenilin-1 exists in both pre- and post-Golgi compartments and recycles via COPI-coated membranes. *Traffic.* 4:553–565.

Rumbaugh, G., J.P. Adams, J.H. Kim, and R.L. Huganir. 2006. SynGAP regulates synaptic strength and mitogen-activated protein kinases in cultured neurons. *Proc. Natl. Acad. Sci. USA.* 103:4344–4351.

Saura, C.A., S.Y. Choi, V. Beglopoulos, S. Malkani, D. Zhang, B.S. Shankaranarayana Rao, S. Chattarji, R.J. Kelleher III, E.R. Kandel, K. Duff, et al. 2004. Loss of presenilin function causes impairments of memory and synaptic plasticity followed by age-dependent neurodegeneration. *Neuron.* 42:23–36.

Scheff, S.W., D.A. Price, F.A. Schmitt, and E.J. Mufson. 2006. Hippocampal synaptic loss in early Alzheimer's disease and mild cognitive impairment. *Neurobiol. Aging.* 27:1372–1384.

Tabata, T., T. Sato, J. Kuromitsu, and Y. Oda. 2007. Pseudo internal standard approach for label-free quantitative proteomics. *Anal. Chem.* 79:8440–8445.

Tashiro, A., and R. Yuste. 2004. Regulation of dendritic spine motility and stability by Rac1 and Rho kinase: evidence for two forms of spine motility. *Mol. Cell. Neurosci.* 26:429–440.

Van de Ven, T.J., H.M. VanDongen, and A.M. VanDongen. 2005. The nonkinase phorbol ester receptor α1-chimerin binds the NMDA receptor NR2A subunit and regulates dendritic spine density. *J. Neurosci.* 25:9488–9496.

Vetrivel, K.S., H. Cheng, W. Lin, T. Sakurai, T. Li, N. Nukina, P.C. Wong, H. Xu, and G. Thinakaran. 2004. Association of γ-secretase with lipid rafts in post-Golgi and endosome membranes. *J. Biol. Chem.* 279:44945–44954.

Walsh, D.M., and D.J. Selkoe. 2004. Deciphering the molecular basis of memory failure in Alzheimer's disease. *Neuron.* 44:181–193.

Xie, Z., D.P. Srivastava, H. Photowala, L. Kai, M.E. Cahill, K.M. Woolfrey, C.Y. Shum, D.J. Surmeier, and P. Penzes. 2007. Kalirin-7 controls activity-dependent structural and functional plasticity of dendritic spines. *Neuron.* 56:640–656.

Zhao, L., Q.L. Ma, F. Calon, M.E. Harris-White, F. Yang, G.P. Lim, T. Morihara, O.J. Ubeda, S. Ambegaokar, J.E. Hansen, et al. 2006. Role of p21-activated kinase pathway defects in the cognitive deficits of Alzheimer disease. *Nat. Neurosci.* 9:234–242.